Applied Physics B
Lasers and Optics

Self-referencable frequency comb from a 170-fs, 1.5-µm solid-state laser oscillator

M.C. Stumpf · S. Pekarek · A.E.H. Oehler · T. Südmeyer · J.M. Dudley · U. Keller

Abstract We report measurement of the first carrier-envelope offset (CEO) frequency signal from a spectrally broadened ultrafast solid-state laser oscillator operating in the 1.5 µm spectral region. The f-to-$2f$ CEO frequency beat signal is 49 dB above the noise floor (100-kHz resolution bandwidth) and the free-running linewidth of 3.6 kHz is significantly better than typically obtained by ultrafast fiber laser systems. We used a SESAM mode-locked Er:Yb:glass laser generating 170-fs pulses at a 75 MHz pulse repetition rate with 110-mW average power. It is pumped by one standard telecom-grade 980-nm diode consuming less than 1.5 W of electrical power. Without any further pulse compression and amplification, a coherent octave-spanning frequency comb is generated in a polarization-maintaining highly-nonlinear fiber (PM-HNLF). The fiber length was optimized to yield a strong CEO frequency beat signal between the outer Raman soliton and the spectral peak of the dispersive wave within the supercontinuum. The polarization-maintaining property of the supercontinuum fiber was crucial; comparable octave-spanning supercontinua from two non-PM fibers showed higher intensity noise and poor coherence. A stable CEO-beat was observed even with pulse durations above 200 fs. Achieving a strong CEO frequency signal from relatively long pulses with moderate power levels substantially relaxes the demands on the driving laser, which is particularly important for novel gigahertz diode-pumped solid-state and semiconductor lasers.

1 Introduction

Self-referenced frequency combs from passively mode-locked femtosecond lasers offer a phase-stable link between optical and microwave frequencies [1–3]. The extremely high measurement accuracy of such combs has enabled significant progress in areas such as precision metrology and spectroscopy [2, 4]. To date, most applications have used frequency combs generated by either Ti:Sapphire or fiber lasers. Ti:Sapphire laser oscillators were the first lasers investigated for self-referenced frequency comb generation [1–3], and many different schemes have been proposed using, for example, an f-to-$2f$ or $2f$-to-$3f$ frequency beat signal [1]. Initially the octave-spanning spectrum required for the f-to-$2f$ frequency beat signal was only obtainable with additional spectral broadening in an external fiber [2, 3]. More recently, CEO-stabilized Ti:Sapphire frequency comb systems have been widely employed because of their excellent low-noise performance [5], operation at high repetition rates [6], and the possibility to generate an octave-spanning spectrum directly from the laser with improved intracavity dispersion management [7]. Unfortunately, Ti:Sapphire lasers have several drawbacks, such as the lack of direct diode-pumping, a relatively low overall system reliability, a limited spectral coverage, and (last but not least) high cost. This has limited their impact for many application areas and strongly motivated research into alternative approaches to generating compact frequency combs.

In this context, the demonstration of CEO-stabilized femtosecond fiber lasers has been a breakthrough [8], because these systems can be integrated into a small package and

M.C. Stumpf · S. Pekarek (✉) · A.E.H. Oehler · T. Südmeyer · U. Keller
ETH Zurich, Physics Department, Institute of Quantum Electronics, Wolfgang-Pauli-Strasse 16, 8093 Zurich, Switzerland
e-mail: spekarek@phys.ethz.ch
Fax: +41-44-6331059

J.M. Dudley
Institut FEMTO-ST, UMR 6174 CNRS-Université de Franche-Comté, 25030 Besançon cedex, France

Fig. 1 Overview of the experimental approach: spectral broadening of the laser output in a polarization-maintaining highly-nonlinear fiber (PM-HNLF) is sufficient for CEO frequency detection with an f-to-$2f$ interferometer
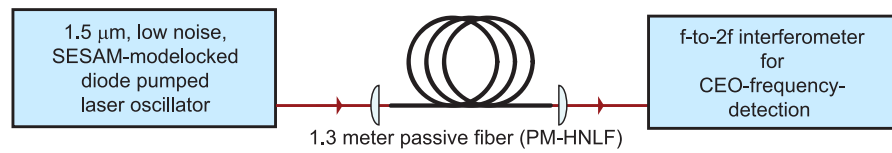
are considerably cheaper and more reliable than Ti:Sapphire systems. Furthermore, they can access the important telecom 1.5-μm spectral region, enabling the usage of standard telecom optics and applications such as long-range fiber distribution of frequency references. However, noise suppression and operation at multi-gigahertz repetition rates are more challenging than for Ti:Sapphire systems. Femtosecond fiber oscillators can show a considerable amount of excess noise [8–14], which arises from the spontaneous emission, the low cavity quality factor, and large intracavity nonlinearities [15]. Even at quantum-limited noise performance, fiber lasers can easily exhibit significant timing-jitter, which is a challenge for stable frequency comb generation [16]. It is therefore important to implement efficient noise suppression schemes [17–20]. Furthermore, repetition rate scaling in fundamentally mode-locked fiber lasers is challenging. Harmonic modelocking, for which more than one pulse is running within one cavity round trip, usually suffers from significant instabilities such as pulse dropout. A major breakthrough was the recent demonstration of a fundamentally mode-locked femtosecond fiber laser with a repetition rate of 1 GHz [21]. However, this is still significantly lower than the 10 GHz obtained from a mode-locked 40-fs Ti:Sapphire laser [22].

In this study, we focus on diode-pumped solid-state lasers (DPSSLs), which are a promising alternative to overcome many of these drawbacks. Self-starting and reliable femtosecond pulse formation is achieved by passive modelocking with a semiconductor saturable absorber mirror (SESAM, [23, 24]). In terms of cost-efficiency and reliability, their performance is similar or better than of femtosecond fiber oscillators, and furthermore, they can access higher average power levels [25, 26]. In addition, femtosecond DPSSLs also have low intrinsic noise which makes them well-suited for optical frequency comb applications. However, only a few frequency combs have been demonstrated with DPSSLs even though a large number of femtosecond bulk laser oscillators have been demonstrated [27]. The first CEO frequency measurement from a DPSSL used Cr:LiSAF as the gain material operating at a center wavelength of 894 nm [28]. The 115-mW output power in 57-fs pulses at 93 MHz repetition rate was sufficient to generate an octave-spanning spectrum from 530 to 1060 nm. The resulting CEO frequency signal had 40 dB signal-to-noise and low bandwidth, but the system had to rely on Kerr-

lens-modelocking, which is a challenge for "real-world" applications outside controlled laboratory environments. The second DPSSL-based CEO frequency measurement used an Yb:KYW femtosecond laser operating at 1030 nm [29]. In this system, the 290-fs pulses from the laser oscillator were first amplified and spectrally broadened with an Yb-doped fiber amplifier and then compressed to 80 fs before the supercontinuum was generated. The resulting CEO-beat had 34 dB signal-to-noise and low bandwidth.

Here we present the first CEO frequency signal measurement using a femtosecond DPSSL operating in the telecom 1.5-μm spectral region. Self-starting and reliable pulse formation is achieved by a SESAM, and the laser generates pulses as short as 170 fs at 75 MHz pulse repetition rate and with an average power of 110 mW. The pulses of the low-noise laser are directly launched into a polarization-maintaining highly-nonlinear fiber (PM-HNLF). Without any further pulse compression and amplification, an octave-spanning supercontinuum is generated, and the CEO frequency signal is detected by an f-to-$2f$ interferometric technique [1] (Fig. 1). Our Er:Yb:glass laser achieves high signal-to-noise ratio and lower bandwidth than free-running fiber oscillators.

2 The femtosecond Er:Yb:glass oscillator

A passively mode-locked femtosecond Er:Yb:glass oscillator has several important advantages. It can be pumped directly with telecom grade laser diodes enabling highly reliable, efficient and stable laser operation. The spectral coverage of the Er:Yb:glass gain bandwidth is well suited for operation in the telecom C-band [30]. In Fig. 2, the schematic of our laser oscillator is shown. It is an improved version of a previous laser which achieved 200-fs pulses with 100 mW average power at a repetition rate of 75 MHz [31]. The main change in this present work was the implementation of a more powerful pump diode (600 mW). A total negative dispersion of -2000 fs^2 per cavity roundtrip is introduced by ten dispersive mirrors. The laser achieves 170-fs pulses with an average power of 110 mW at the same repetition rate (Fig. 3). The pulses were transform-limited with time-bandwidth product 0.31. Note that the measured autocorrelation function of the pulses was very well fitted assuming a sech^2-pulse profile typically observed for stable soliton
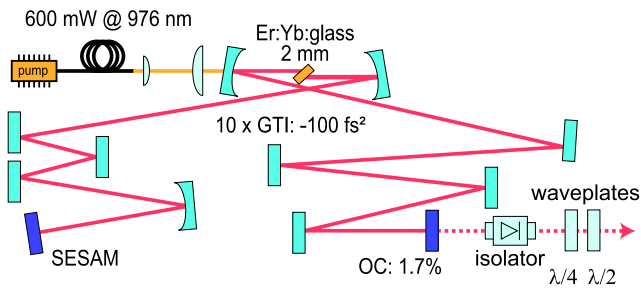
Fig. 2 Design of the ultrafast Er:Yb:glass oscillator. SESAM: semiconductor saturable absorber mirror; GTI: high reflective Gires–Tournois interferometer type mirror, dispersion -100 fs^2; OC: output coupler, transmission 1.7%. The laser output passes through an isolator for protection against back reflections, and waveplates for polarization control

modelocking and for which the pulse duration is determined by the amount of negative dispersion and self-phase modulation [32]. Thus the duration of the output pulses can also be adjusted with the pump power according to Eq. (21) in Ref. [32]. As explained later, this can be used to control the CEO frequency.

The key advantage of this setup for frequency comb applications is the excellent stability of the laser. At higher repetition rates, SESAM mode-locked Er:Yb:glass-lasers have demonstrated close to quantum noise limited performance [33]. A detailed analysis shows that resonators with higher Q-factors have a lower quantum noise limit [15]. Thus, the oscillator was designed for minimum intracavity loss. The output coupling is only 1.7%, the nonsaturable losses of the SESAM are below 0.2% measured with very high accuracy [34], and the transmission of one (GTI)-mirror is below 0.01%. Therefore the total roundtrip loss of the cavity is well below 3%, leading to a substantially higher Q-factor and a significantly lower quantum noise limit than typical fiber lasers. The excellent noise performance of this laser is verified by relative intensity noise measurements (Fig. 6; see [31] for a description of the measurement routine).
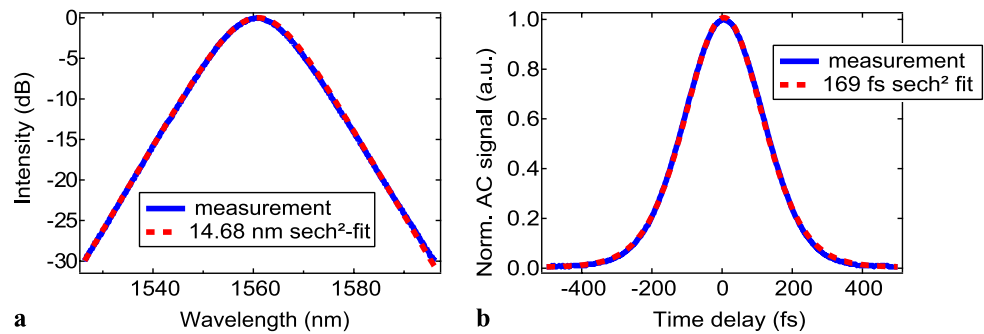
3 Supercontinuum generation

In order to use the f-to-$2f$ interferometer scheme for CEO frequency detection, it is essential to provide a phase-stable, octave-spanning spectrum from the laser pulse train. So far, only Ti:Sapphire oscillators can achieve an octave-spanning spectrum directly from the oscillator [7]. Other femtosecond lasers rely on strong spectral broadening in fibers under conditions that preserve essential phase coherence [35]. For example, it has been shown that the coherence might strongly degrade at longer input pulse durations [36, 37]. In addition, high spectral power densities separated by an octave are required to achieve good signal strength of the f-to-$2f$ frequency beat signal that determines the CEO frequency. These issues are particularly challenging for the rather long pulse durations of 170 to 300 fs available from our Er:Yb:glass laser, and thus required a detailed investigation and optimization of the nonlinear spectral broadening.

Both octave-spanning broadening and excellent coherence were achieved using a state-of-the-art dispersion-flattened, polarization-maintaining, highly-nonlinear fiber (manufactured by OFS Fitel Denmark [38, 39]). The fiber was fabricated with an all-solid design by the Modified Chemical Vapor Deposition (MCVD) technique. Polarization maintenance (PM) is introduced by an elliptical core while the nonlinearity is enhanced through Ge-doping. The fiber has a specified beat length of 10.4 mm and an effective area of 12.7 μm^2, giving an estimate of 10.5 W/km for the nonlinear coefficient. A measured dispersion curve is plotted in Fig. 4. By optimizing the input polarization and choosing an appropriate fiber length of 1.3 m we could shift the outer spectral peaks to be separated exactly by one octave (Fig. 4). The supercontinuum had an average power of 50 mW and it was polarized and stable.

In order to gain more insight into the dynamics of supercontinuum generation, we performed numerical simulations based on a generalized nonlinear Schrödinger equation. The pulse propagation in the PM-HNLF was calculated with a split-step algorithm including the effects of dispersion, self-phase modulation, self-steepening, and Raman effect [36, 40]. Using the fiber parameters and the laser parameters from above, a cubic extrapolation of the measured dispersion slope (D parameter), and assuming a coupling efficiency of 70% into the fiber, we could achieve excellent agreement with our measured spectra (Fig. 4). The simulations reveal that the supercontinuum generation can be well explained with the model of high-order soliton fission as is expected due to the seeding in the anomalous dispersion regime (Fig. 5) [36]. Soliton fission occurs after about 10 cm of PM-HNLF. Afterwards, Raman scattering generates red-shifted soliton pulses at the long-wavelength part of the spectrum, which in turn create new spectral components on the short-wavelength edge through resonant energy transfer. After only 20 cm, the supercontinuum has nearly reached its final spectral width. In the following section of the fiber, only slow broadening up to the final supercontinuum bandwidth takes place, mainly due to increased Raman soliton self-frequency shift. A particular benefit of the supercontinuum process that is not widely appreciated is the fact that the outer Raman soliton has high peak power, which gives rise to good efficiency at the second harmonic generation (SHG) in the subsequent f-to-$2f$-interferometer and thereby contributes to the excellent signal-to-noise ratio (Fig. 5). Although supercontinuum generation can readily generate the necessary octave of bandwidth for f-to-$2f$ interometery, high-contrast CEO-beat signal detection also

Fig. 3 Pulses from the SESAM mode-locked Er:Yb:glass laser as shown in Fig. 2: spectrum (**a**) and autocorrelation trace (**b**) of the generated pulses directly after the oscillator plotted with fits for a sech^2-pulse

Fig. 4 Generated supercontinuum. *Blue line*: measured spectrum of the 1.3-meter PM-HNLF; *red line*: simulated spectrum of the 1.3-meter PM-HNLF; *green line*: unbroadened laser spectrum; *gray line*: dispersion profile of the PM-HNLF used in the simulation; *black dots*: measured dispersion profile [39]
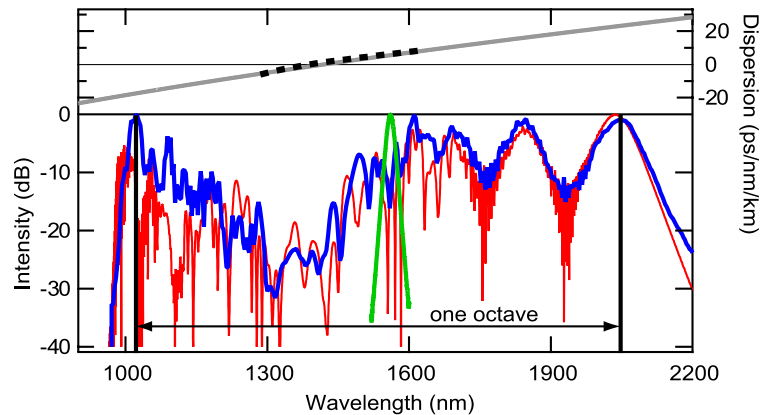
requires intensity and phase stability across the supercontinuum spectrum [41]. For our parameters, the input soliton number N is approximately 6, which suggests that coherent supercontinuum broadening should be possible [36] and this was checked explicitly by carrying out multiple simulations in the presence of noise to verify that unity coherence across the octave bandwidth was indeed maintained [37].

While a direct measure of the coherence in experiments is difficult [35], we evaluated different fibers and measured the relative intensity noise (RIN) of their supercontinuum as there is a general tendency towards higher intensity noise when the coherence is poor [37]. In consequence, a fiber with low intensity noise is a good candidate for a coherent supercontinuum process. Because of the low noise levels, a direct detection of the photocurrent with an RF-analyzer is not suitable for lower frequencies and a time-domain measurement scheme with a resolution bandwidth of only 1 was applied (Fig. 6a) as described in [31]. At higher noise frequencies, an RF-analyzer was used with a resolution bandwidth of 10 kHz (Fig. 6b) and 100 kHz (Fig. 6c), respectively. All measurements were recorded with the same average photocurrent and have afterwards been normalized to dBc/Hz. For the measurement of the instrument noise floor, the photodiode was exposed to an incandescent lamp generating the same photocurrent. The measurements have been performed with a standard InGaAs photodiode with a peak sensitivity at the laser's center wavelength and good sensitivity at the short-wavelength range of the supercon-
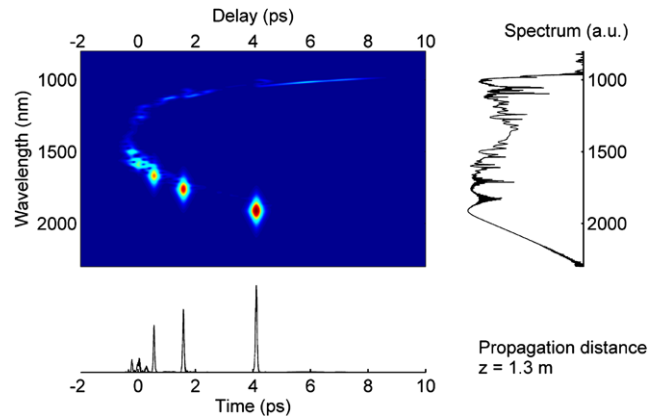
Fig. 5 Simulated supercontinuum spectrogram projected onto the temporal and spectral intensity distribution revealing the underlying dynamics [36]

tinuum. Although the RIN levels can strongly vary across the entire SC spectrum [41], it is very unlikely that instabilities would only occur in the long-wavelength spectral region >1700 nm outside the sensitivity range of the photodiode. We tested three different fibers, each generating an octave-spanning supercontinuum at the displayed fiber length. A comparison reveals significant differences between their RIN levels.

For high frequencies, the RIN of the laser and the PM-HNLF approach the system noise floor: above ~200 kHz, the laser and the PM-HNLF show shot-noise-limited per-
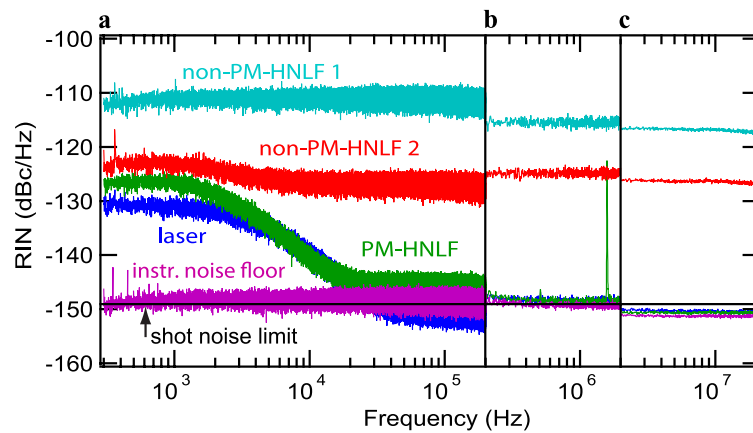
Fig. 6 Measured relative intensity noise (RIN). RIN of our ultrafast Er:Yb:glass oscillator (*dark blue line*); the supercontinuum generated with the non-PM-HNLF 1 (*light blue line*), the non-PM-HNLF 2 (*red line*), the PM-HNLF (*green line*), and the instrument noise floor (*purple line*). The low frequency range (**a**) was recorded with a resolution bandwidth of 1 Hz, the frequency range (**b**) with 10 kHz, and the frequency range (**c**) with 100 kHz, respectively. The average photocurrent was constant at all measurements and corresponds to the indicated shot-noise level at −149 dBc/Hz (*black horizontal line*)

**Fig. 7** The f-to-$2f$ interferometer used for CEO frequency detection after the PM-HNLF
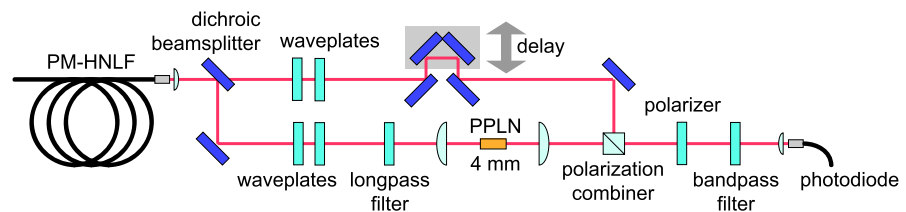
formance at approximately −150 dBc, which is lower than reported for a low-noise fiber laser [42]. The single peak of the PM-HNLF at 1.6 MHz is probably caused by an insufficient shielding of the detection system. In the frequency range above 200 kHz, the non-PM fibers obviously generate substantial noise power compared to the PM-fiber. Hence, one would expect better coherence from the PM-fiber. Indeed, we have not been able to generate a CEO-beat from our laser with the non-PM-HNLF 1 at all, although its spectral bandwidth and signal strength would allow for CEO frequency detection. Only by launching much shorter 65-fs pulses from an amplified 1.5-µm fiber laser system into this fiber, CEO-beats could be generated at low signal levels revealing crucial sensitivity to the input polarization. In contrast, the PM-HNLF allows for stable CEO-beat generation even from the moderate pulse durations of the Er:Yb:glass oscillator. Here, the supercontinuum generation is very stable against perturbations on the input polarization or on the fiber itself. This result suggests the occurrence of chaotic nonlinear polarization rotation in the non-PM-HNLFs causing crucial instabilities during supercontinuum generation [43]. Consequently, the coherence decays and excess intensity noise is observed. With a PM-fiber these instabilities are eliminated. The fixed polarization obviously ensures stable interaction of the strong electrical fields supporting a coherent, octave-spanning supercontin-

uum at much longer pulse durations where non-PM-HNLFs do not generate a CEO frequency signal above the noise floor. In addition, the PM-HNLF has generated an octave-spanning spectrum at much shorter fiber length, even though it has very similar nonlinear and dispersive characteristics compared to the non-PM-HNLF 2. These experimental findings need further theoretical investigations and are very exciting also for the future prospect of more compact gigahertz frequency combs.

4 CEO frequency detection

After supercontinuum generation in the PM-HNLF, we detected the CEO frequency with an f-to-$2f$ interferometer (Fig. 7) [1]. By frequency-doubling of the long-wavelength Raman soliton and interfering it with the short-wavelength peak of the supercontinuum, a beat signal is produced which represents the absolute offset frequency of the comb. The implementation of the f-to-$2f$-interferometer is standard. The supercontinuum is separated by a dichroic beam-splitter and combined again after the long-wavelength signal has been frequency-doubled. At room temperature, a 4-mm long periodically poled lithium niobate (PPLN) crystal with a poling period of 31.1 µm generates a second harmonic signal with 8 nm bandwidth at 1025 nm. We achieved an average

Fig. 8 RF spectrum with CEO frequency over a large 80-MHz span (RB = 100 kHz, video bandwidth 1 kHz). (**b**) Magnified and centered RF spectrum of the left CEO frequency peak with a squared-Lorentzian fit of 3.6 kHz FWHM ($RB = 1$ kHz, video bandwidth 300 Hz)
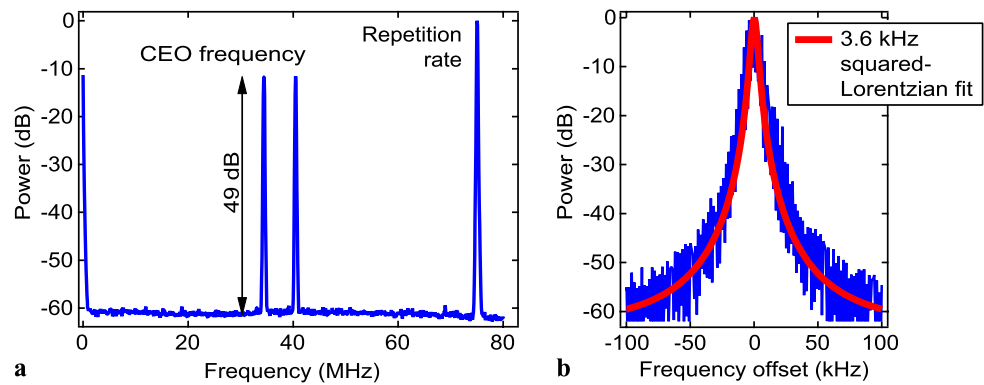
frequency-doubled power of up to 0.5 mW corresponding to a conversion efficiency of 10% of the available supercontinuum power in a 16 nm bandwidth at 2050 nm. This efficiency is essential for a good signal-to-noise ratio and has mainly been achieved because of the high peak power from the outermost Raman soliton. The waveplates inside the interferometer set the correct polarization for PPLN-crystal and the combiner. After the combiner an adjustable polarizer projects both fields into the same plane and also balances the power of both interferometer arms for optimal contrast. Additionally, the contrast is increased by the band-pass filter removing the background out of the SHG-bandwidth. The signal is finally detected with a fiber coupled photodiode and monitored with an electrical spectrum analyzer.

5 Results

When the delay between both interferometer arms is well adjusted, a clear CEO-beat signal is obtained. Figure 8a shows the corresponding frequency spectrum over an 80-MHz span. The main peak at 75 MHz is the pulse repetition rate, and the CEO frequency appears as sidebands around DC and the first harmonic of the pulse train signal. The signal-to-noise ratio (SNR) is 49 dB in a 100-kHz resolution bandwidth (RB), which is significantly better than typically obtained by fiber oscillators [8–14], and substantially higher than the typical 30 dB required for standard stabilization electronics. Even more important is the bandwidth of the CEO frequency variations since it reflects the intrinsic stability of the underlying laser oscillator. For further analysis, a magnified spectrum of the first CEO-beat is shown in Fig. 8b together with a squared-Lorentzian fit of 3.6 kHz FWHM. This is to our knowledge the narrowest CEO frequency linewidth of a free-running laser in the 1.5-μm regime. A state-of-the-art amplified fiber oscillator system is presented by Hartl et al. in [14]. Its free-running CEO frequency distribution fits well

to a Lorentzian function, not a squared-Lorentzian function as observed in our measurements. This suggests that a different noise mechanism is dominant. In addition, our CEO frequency linewidth is more than 10 times narrower at FWHM and even 40 times narrower at the −30 dB level.

It is common to stabilize optical frequency combs by active feedback from a phase-locked loop (PLL), which reduces their linewidth by orders of magnitude [14]. The presented system has not yet been stabilized, but considering the high intrinsic stability and the excellent signal strength we expect that stabilization will be straightforward. A lower control bandwidth by the feedback-loop system is required, and therefore also excellent performance after stabilization is expected. The free-running CEO frequency is very stable and not subject to constant drifts or sudden shifts as long as the pump current is stable. We can shift the CEO frequency continuously with the pump current at a rate of 260 kHz/mA. It is even possible to shift the CEO frequency by more than 30 MHz using this control mechanism. Hence, the pump current alone can be used for CEO frequency stabilization.

It is interesting that a CEO frequency signal can still be observed at a large reduction of pump power. Less pump power decreases the pulse energy and increases the pulse duration for soliton modelocking (as explained above) and therefore even more strongly reducing the peak power of the pulse. One would expect strong effects on the spectrum and the coherence of the supercontinuum. However, the observed CEO frequency signal strength proves that this is not the case. In fact, a strong CEO signal with more than 30 dB SNR is maintained up to pulse durations of 260 fs. This is remarkable, because CEO frequency signals are usually generated from significantly shorter pulses. To the best of our knowledge, we observed the first experimental demonstration of a coherent, octave-spanning supercontinuum from pulse durations above 120 fs launched directly into a highly-nonlinear fiber [44]. This achievement substantially lowers the demands on the mode-locked lasers for self-referenced stable frequency combs.

6 Conclusion and outlook

In conclusion, we have demonstrated the first direct CEO frequency detection from an ultrafast Er:Yb:glass laser oscillator using a standard f-to-$2f$ interferometer [1]. The SESAM-mode-locked, diode-pumped laser uses a high-Q cavity which results in low-noise operation. A coherent, octave-spanning supercontinuum is generated by nonlinear spectral broadening in a polarization-maintaining highly-nonlinear fiber (PM-HNLF) without further pulse compression and pulse amplification. We observe an improvement of more than an order of magnitude in the free-running CEO frequency linewidth when compared to free-running femtosecond fiber laser systems operating in this spectral region.

From a physical perspective, the high SNR can be attributed to supercontinuum generation with low excess noise despite the tremendous spectral broadening. The extremely low linewidth of the free-running CEO signal relates to low optical phase noise due to the high-Q cavity. Significantly, an unexpected and surprising result was that we could obtain a very stable CEO frequency even with rather long pulses of above 250 fs duration. A more detailed investigation with non-PM fibers under similar conditions suggests that the polarization-maintaining feature of the HNLF was the enabling key technology improvement. Further theoretical investigations that take into account a possibly chaotic polarization rotation and its effect on the CEO frequency noise will be expected to provide further insight into these observations. By now, we could already achieve excellent agreement between the measured and simulated supercontinuum spectrum and could optimize the fiber length to increase the spectral signal strength at the opposite frequencies separated by an octave within the supercontinuum.

We expect that this result will have a significant impact in the future development of more compact stable frequency combs because the relatively long pulse durations of more than 250 fs strongly relax the requirements on the mode-locked lasers. This will become even more important for gigahertz pulse repetition rates. For example, picosecond diode-pumped solid-state lasers have successfully been demonstrated up to 160 GHz at 1.06 μm [45] and up to 100 GHz at 1.5 μm [46, 47]. The extension of these results to the femtosecond regime looks very promising considering for example the large progress on Yb-doped solid-state laser crystals that support sub-100 fs pulses [26, 27, 48] and the development of optimized SESAMs for gigahertz operation [49, 50]. Furthermore, high average power ultrafast gigahertz lasers may become even more compact and cost-effective with the recent development of SESAM mode-locked optically-pumped semiconductor disk lasers (also referred to as optically-pumped vertical external cavity surface emitting lasers, OP-VECSELs) [51].

These lasers typically operate in the multi-gigahertz repetition rate regime, and pulse durations of 260 fs were already achieved [52]. An even more compact wafer-scalable approach comprises the optically-pumped mode-locked integrated external-cavity surface emitting lasers (MIXSELs) [53, 54], for which SESAM and semiconductor gain structure are integrated into one single element. The advantage of DPSSLs, VECSELs, and MIXSELs are that they all use high-Q cavities which inherently have significantly less noise than fiber lasers and can be scaled to gigahertz pulse repetition rates. However, achieving extremely short pulse duration at multi-gigahertz operation is challenging, and a relaxed pulse width requirement for stable self-referenced frequency combs represents a very exciting development for the practical application of these lasers in frequency metrology.

References

1. H.R. Telle, G. Steinmeyer, A.E. Dunlop, J. Stenger, D.H. Sutter, U. Keller, Appl. Phys. B **69**, 327 (1999)
2. S.A. Diddams, D.J. Jones, J. Ye, S. Cundiff, J.L. Hall, J.K. Ranka, R.S. Windeler, R. Holzwarth, T. Udem, T.W. Hänsch, Phys. Rev. Lett. **84**, 5102 (2000)
3. D.J. Jones, S.A. Diddams, J.K. Ranka, A. Stentz, R.S. Windeler, J.L. Hall, S.T. Cundiff, Science **288**, 635 (2000)
4. T. Udem, R. Holzwarth, T.W. Hänsch, Nature **416**, 233 (2002)
5. L.-S. Ma, Z. Bi, A. Bartels, L. Robertsson, M. Zucco, R.S. Windeler, G. Wilpers, C. Oates, L. Hollberg, S.A. Diddams, Science **303**, 1843 (2004)
6. A. Bartels, D. Heinecke, S.A. Diddams, Opt. Lett. **33**, 1905 (2008)
7. H.M. Crespo, J.R. Birge, E.L. Falcão-Filho, M.Y. Sander, A. Benedick, F.X. Kärtner, Opt. Lett. **33**, 833 (2008)
8. B.R. Washburn, S.A. Diddams, N.R. Newbury, J.W. Nicholson, M.F. Yan, C.G. Jørgensen, Opt. Lett. **29**, 250 (2004)
9. F.-L. Hong, K. Minoshima, A. Onae, H. Inaba, H. Takada, A. Hirai, H. Matsumoto, T. Sugiura, M. Yoshida, Opt. Lett. **28**, 1516 (2003)
10. F. Tauser, A. Leitenstorfer, W. Zinth, Opt. Express **11**, 594 (2003)
11. T.R. Schibli, K. Minoshima, F.L. Hong, H. Inaba, A. Onae, H. Matsumoto, I. Hartl, M.E. Fermann, Opt. Lett. **29**, 2467 (2004)
12. F. Adler, K. Moutzouris, A. Leitenstorfer, H. Schnatz, B. Lipphardt, G. Grosche, F. Tauser, Opt. Express **12**, 5872 (2004)
13. B. Washburn, R. Fox, N. Newbury, J. Nicholson, K. Feder, P. Westbrook, C. Jørgensen, Opt. Express **12**, 4999 (2004)
14. I. Hartl, G. Imeshev, M.E. Fermann, C. Langrock, M.M. Fejer, Opt. Express **13**, 6490 (2005)
15. R. Paschotta, A. Schlatter, S.C. Zeller, H.R. Telle, U. Keller, Appl. Phys. B **82**, 265 (2006)

16. O. Prochnow, R. Paschotta, E. Benkler, U. Morgner, J. Neumann, D. Wandt, D. Kracht, Opt. Express **17**, 15525 (2009)
17. E. Benkler, H.R. Telle, A. Zach, F. Tauser, Opt. Express **13**, 5662 (2005)
18. W.C. Swann, J.J. McFerran, I. Coddington, N.R. Newbury, I. Hartl, M.E. Fermann, P.S. Westbrook, J.W. Nicholson, K.S. Feder, C. Langrock, M.M. Fejer, Opt. Lett. **31**, 3046 (2006)
19. J.J. McFerran, W.C. Swann, B.R. Washburn, N.R. Newbury, Appl. Phys. B **86**, 219 (2007)
20. N.R. Newbury, W.C. Swann, J. Opt. Soc. Am. B **24**, 1756 (2007)
21. I. Hartl, H.A. McKay, R. Thapa, B.K. Thomas, A. Ruehl, L. Dong, M.E. Fermann, in *Proceedings of Advanced Solid-State Photonics* (Denver, Colorado, USA, 2009), p. MF9
22. A. Bartels, D. Heinecke, S.A. Diddams, Science **326**, 681 (2009)
23. U. Keller, D.A.B. Miller, G.D. Boyd, T.H. Chiu, J.F. Ferguson, M.T. Asom, Opt. Lett. **17**, 505 (1992)
24. U. Keller, K.J. Weingarten, F.X. Kärtner, D. Kopf, B. Braun, I.D. Jung, R. Fluck, C. Hönninger, N. Matuschek, J. Aus der Au, IEEE J. Sel. Top. Quantum Electron. **2**, 435 (1996)
25. U. Keller, Nature **424**, 831 (2003)
26. T. Südmeyer, C. Kränkel, C.R.E. Baer, O.H. Heckl, C.J. Saraceno, M. Golling, R. Peters, K. Petermann, G. Huber, U. Keller, Appl. Phys. B **97**, 281 (2009)
27. U. Keller, in *Landolt-Börnstein. Laser Physics and Applications. Subvolume B: Laser Systems. Part I*, ed. by G. Herziger, H. Weber, R. Proprawe (Springer, Heidelberg, 2007), pp. 33–167
28. R. Holzwarth, M. Zimmermann, T. Udem, T.W. Hänsch, P. Russbüldt, K. Gäbel, R. Poprawe, J.C. Knight, W.J. Wadsworth, P.S.J. Russell, Opt. Lett. **26**, 1376 (2001)
29. S.A. Meyer, J.A. Squier, S.A. Diddams, Eur. Phys. J. D **48**, 19 (2008)
30. G.J. Spühler, L. Krainer, E. Innerhofer, R. Paschotta, K.J. Weingarten, U. Keller, Opt. Lett. **30**, 263 (2005)
31. M.C. Stumpf, S.C. Zeller, A. Schlatter, T. Okuno, T. Südmeyer, U. Keller, Opt. Express **16**, 10572 (2008)
32. F.X. Kärtner, I.D. Jung, U. Keller, IEEE J. Sel. Top. Quantum Electron. **2**, 540 (1996)
33. A. Schlatter, B. Rudin, S.C. Zeller, R. Paschotta, G.J. Spühler, L. Krainer, N. Haverkamp, H.R. Telle, U. Keller, Opt. Lett. **30**, 1536 (2005)
34. D.J.H.C. Maas, B. Rudin, A.-R. Bellancourt, D. Iwaniuk, S.V. Marchese, T. Südmeyer, U. Keller, Opt. Express **16**, 7571 (2008)
35. B. Schenkel, R. Paschotta, U. Keller, J. Opt. Soc. Am. B **22**, 687 (2005)
36. J.M. Dudley, G. Genty, S. Coen, Rev. Mod. Phys. **78**, 1135 (2006)
37. J.M. Dudley, S. Coen, Opt. Lett. **27**, 1180 (2002)
38. L. Grüner-Nielsen, in *Proceedings of IEEE LEOS Winter Topicals* (Innsbruck, Austria, 2009), p. TuC4.2 (invited)
39. L. Grüner-Nielsen, B. Pálsdóttir, in *Proceedings of Fiber Lasers V: Technology, Systems, and Applications* (SPIE, San Jose, 2008), pp. 68731B–68738
40. G.P. Agrawal, *Nonlinear Fiber Optics* (Academic Press, San Diego, 2001)
41. K.L. Corwin, N.R. Newbury, J.M. Dudley, S. Coen, S.A. Diddams, B.R. Washburn, K. Weber, R.S. Windeler, Appl. Phys. B **77**, 269 (2003)
42. J. Chen, J.W. Sickler, E.P. Ippen, F.X. Kärtner, Opt. Lett. **32**, 1566 (2007)
43. Z. Zhu, T.G. Brown, J. Opt. Soc. Am. B **21**, 249 (2004)
44. J.W. Nicholson, A.D. Yablon, M.F. Yan, P. Wisk, R. Bise, D.J. Trevor, J. Alonzo, T. Stockert, J. Fleming, E. Monberg, F. Dimarcello, J. Fini, Opt. Lett. **33**, 2038 (2008)
45. L. Krainer, R. Paschotta, S. Lecomte, M. Moser, K.J. Weingarten, U. Keller, IEEE J. Quantum Electron. **38**, 1331 (2002)
46. A.E.H. Oehler, T. Südmeyer, K.J. Weingarten, U. Keller, Opt. Express **16**, 21930 (2008)
47. A.E.H. Oehler, T. Südmeyer, K.J. Weingarten, U. Keller, in *Proceedings of Advanced Solid-State Photonics (ASSP)* (Denver, 2009), paper MA4
48. F. Druon, F. Balembois, P. Georges, C. R. Phys. **8**, 153 (2007)
49. D.J.H.C. Maas, A.R. Bellancourt, M. Hoffmann, B. Rudin, Y. Barbarin, M. Golling, T. Südmeyer, U. Keller, Opt. Express **16**, 18646 (2008)
50. G.J. Spühler, K.J. Weingarten, R. Grange, L. Krainer, M. Haiml, V. Liverini, M. Golling, S. Schon, U. Keller, Appl. Phys. B **81**, 27 (2005)
51. U. Keller, A.C. Tropper, Phys. Rep. **429**, 67 (2006)
52. K.G. Wilcox, Z. Mihoubi, G.J. Daniell, S. Elsmere, A. Quarterman, I. Farrer, D.A. Ritchie, A. Tropper, Opt. Lett. **33**, 2797 (2008)
53. A.-R. Bellancourt, D.J.H.C. Maas, B. Rudin, M. Golling, T. Südmeyer, U. Keller, IET Optoelectron. **3**, 61 (2009)
54. D.J.H.C. Maas, A.-R. Bellancourt, B. Rudin, M. Golling, H.J. Unold, T. Südmeyer, U. Keller, Appl. Phys. B **88**, 493 (2007)